THE JOURNAL OF PHYSICAL CHEMISTRY C

Article

pubs.acs.org/JPCC

CVD Growth of Carbon Nanotube Forest with Selective Wall-Number from Fe–Cu Catalyst

Pan Li and Jin Zhang*

Center for Nanochemistry, Beijing Science and Engineering Center for Nanocarbons, Beijing National Laboratory for Molecular Sciences, College of Chemistry and Molecular Engineering, Peking University, Beijing 100871, P. R. China

Supporting Information

ABSTRACT: We reported herein the chemical vapor deposition (CVD) growth of vertically aligned carbon nanotubes (CNTs) with selective wall-number using binary Fe–Cu catalysts. High quality single-walled carbon nanotube (SWNT) and double-walled carbon nanotube (DWNT) forests were predominantly produced with selectivity of ~92% and ~85%, respectively. Formation of small catalyst nanoparticles with high areal density and fully reduced state was found key for efficient SWNT growth. Characterization of the catalysts by atomic force microanalysis (AFM) and high resolution transmission electron microscope (HRTEM) showed that the introduction of the proper amount of Cu into the Fe/Al_2O_3 catalyzing system inhibited diffusion of Fe NPs and facilitated the full reduction of Fe catalyst, thus facilitating the selective growth of SWNTs. DWNTs were also obtained by introducing a thick layer of Cu catalyst onto Fe/Al_2O_3. Our work provides a rational way for selective growth of vertically aligned SWNTs and DWNTs, whose remarkable electronic and mechanical properties enable their promising application in nanoelectronics devices.

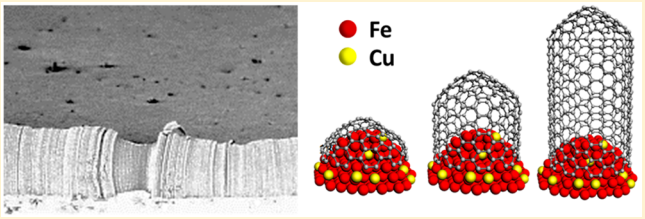

INTRODUCTION

Vertically aligned carbon nanotubes (CNTs), especially single-walled carbon nanotubes (SWNTs) and double-walled carbon nanotubes (DWNTs), have been a subject of tremendous research activities due to their superior mechanical,[1] thermal,[2,3] optical, and electrical properties.[4−6] Because of the considerable advantages of the vertical alignment over random orientation, both SWNT and DWNT forests have great potential as building blocks in high-performance superfibers,[7,8] field emitters,[9,10] light absorbers,[11] and energy and environment related applications.[12,13] It is expected that the list of applications would become even longer if the length, areal density, as well as the wall-number, diameter, and chirality of the CNTs are well-controlled. Pioneer reports have demonstrated the controlled growth of high-quality vertically aligned SWNTs and DWNTs with uniform structures. However, further knowledge on the dependence of CNT structure on specific synthesis factors is still required to realize the controlled growth of CNT forests for application.

Among all the essential structure parameters of CNTs, the wall-number is of special importance owing to the fact that it is the prerequisite to the control of many important properties. For example, the uniqueness of SWNTs, whose defined energy band structures directly correlate to the tube diameters and chiralities, provides a chance to control the electronic properties; when used for field emission, DWNTs are most desirable because they simultaneously have the low threshold voltage of SWNTs and high durability of multiwalled carbon nanotubes (MWNTs).[14] For these reasons, the preferential growth of CNTs with homogeneous wall-number is highly wanted for specific applications.

Recently, the most common and efficient growth system for vertically aligned CNTs (V-CNTs) is chemical vapor deposition (CVD) system, which produces CNTs following a well-recognized vapor–liquid–solid (VLS) mechanism.[6] According to the VLS mechanism, the catalyst serves as seed or template for CNT nucleation and growth. Consequently, catalyst engineering deserves the most attention and effort for the selective growth of V-CNTs. The general rule for catalyst engineering is to obtain catalyst nanoparticles (NPs) with desired areal density, size, and surface properties. To realize this goal, the strategies that have been reported include the following: (i) Choosing proper oxides as supporting layer for the metal catalyst is one strategy. Al_2O_3 has been used as a common supporting layer especially for Fe based catalysts because of the strong $Fe–Al_2O_3$ interaction.[15,16] The addition of a secondary SiO_2 supporting layer was recently found to promote the preferential growth of large-diameter vertically aligned SWNTs (V-SWNTs) by better controlling the size and areal density of Fe catalyst NPs.[17] (ii) Water-assisted super growth is a second strategy.[18] H_2O was identified to have two essential functions. One is etching the excessive amorphous carbon on the catalyst, which helps maintain the active state of the Fe catalyst.[19] The other is to inhibit the diffusion and Ostwald ripening of the metal catalyst.[20] (iii) Development of

Received: December 24, 2015
Revised: May 1, 2016
Published: May 2, 2016

DOI: 10.1021/acs.jpcc.5b12602
J. Phys. Chem. C 2016, 120, 11163−11169

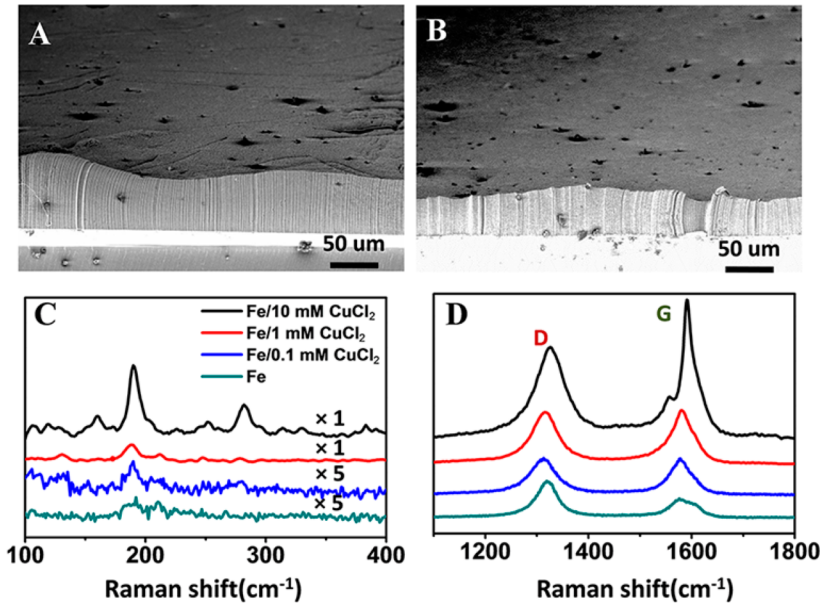

Figure 1. SEM images of vertically aligned CNTs grown on Fe/Al_2O_3 catalyst (A) and Fe/0.1 mM $CuCl_2/Al_2O_3$ catalyst (B). Raman spectra of RBM peaks (C) and the D- and G-band modes (D) of CNTs synthesized on Fe/Al_2O_3 catalyst and $Fe/Cu/Al_2O_3$ catalysts with different amounts of Cu introduced. The spectra were collected with a 633 nm He−Ne laser, and the legends were shared between parts C and D.

binary or even triple metallic catalysts is a third strategy. Fe, Co, and Ni are the most frequently involved metals. The advantage of these catalysts comes from the synergetic effect induced by the interaction between different metal components. For example, due to the stronger interaction between Fe−Pt NPs and the Al_2O_3 supporting layer than that of Fe and Al_2O_3, ultrafine and uniform Fe−Pt NPs were generated and facilitated the selective growth of V-SWNTs and vertically aligned DWNTs (V-DWNTs).[21] Similarly, Fe−Mo,[22] Co−Mo,[23] and Ni−Cr−Fe[24] were used to preferentially grow V-SWNTs and V-DWNTs. The catalyst composition of bimetallic catalysts (Fe−Mn, Fe−Co, Fe−Ni, and Fe−Cu) was also shown to influence the height and chirality distribution of the V-SWNT arrays.[25] This finding suggests that tuning the type and content of each metal in the composite catalyst could be utilized to realize type-selective growth of V-CNT arrays.

Despite enormous research efforts, the exact relationship between the catalyst properties and the nanotube structures and the method for designing catalysts for selective growth of V-CNTs with specific wall-numbers remain elusive. Bimetallic catalysts such as CoMo, CoW, FeCu, FeNi, etc. have been employed for chirality selective growth of horizontal SWNTs for a long time and have been proven very effective.[26−29] The mechanism for how the catalyst composition and structure affect the chirality distribution is deeply investigated.[30,31] Therefore, it is expected that these understandings could also benefit the research on the structure-controlled growth of V-CNTs.

In this work, we used two kinds of $Fe/Cu/Al_2O_3$ catalyst systems to achieve selective growth of V-SWNTs and V-DWNTs, respectively. By tailoring the amount and form of the Cu introduced into Fe/Al_2O_3 system, we demonstrated that both areal density and oxidation state of Fe (Fe−Cu) catalyst can be effectively controlled. Consequently, V-CNTs with specific wall-number predominantly nucleate and grow on catalyst NPs with suitable sizes and oxidation states. A growth model is proposed that considers the facilitated reduction of the catalyst as a critical factor, besides the widely known catalyst size, for the wall-number-controlled synthesis of V-CNTs.

EXPERIMENTAL SECTION

Catalyst Deposition. First, a thin film of 0.8 nm Fe over 10 nm Al_2O_3 was deposited by e-beam evaporation (ULVAC Ei-5) on n-type Si(100) with 300 nm thick oxide layer; then, a different amount of $CuCl_2$ dispersed in ethanol was used as a Cu precursor to make the Fe−Cu catalyst used for V-SWNT growth. The volume of the $CuCl_2$ solution was fixed, and the concentration was varied to adjust the amount of Cu. The Cu precursor solution was spin-coated onto the surface of Fe/Al_2O_3 at 3000 rpm for 1 min. Cu layer and Ni layer were deposited by thermal evaporation onto the 0.8 nm Fe/Al_2O_3 film (ULVAC Ei-5). Quasiatomic layer of Al_2O_3 was deposited by atomic layer deposition (Savannah 100) from trimethylaluminum (TMA) and water. Only one growth cycle was used to get an ultrathin discontinuous Al_2O_3 layer.

V-CNT Growth. The CNT growth was performed in a tube furnace (Lindberg Blue), equipped with a fused-quartz tube with an internal diameter of 22 mm. When the furnace temperature ramped to 750 °C in a mixture of 200 standard cubic centimeters per minute (sccm) Ar and 125 sccm H_2, the catalyst was thermally annealed under the same atmosphere for 5 min. After that, a flow of 30 sccm C_2H_4 was added to start the V-CNT growth. The growth lasted for 15 min and was terminated by turning off the C_2H_4 flow. The furnace was subsequently cooled down to room temperature in the atmosphere of 200 sccm Ar and 40 sccm H_2.

TEM Sample Preparation of Fe (Fe−Cu) NPs for TEM Characterization. The TEM samples were prepared following a procedure reported elsewhere.[21] A 10 or 50 nm thick Al_2O_3 layer was first deposited onto a NaCl single crystal, followed by Fe deposition. For $Fe/Cu/Al_2O_3$ catalyst, $CuCl_2$ deposition was performed after the Fe deposition. The so-formed catalyst film was thermally annealed under 200 sccm Ar and 125 sccm H_2 at 750 °C for 40 min, and then cooled down to room temperature. The NaCl crystal with catalyst was then put

DOI: 10.1021/acs.jpcc.5b12602
J. Phys. Chem. C 2016, 120, 11163−11169

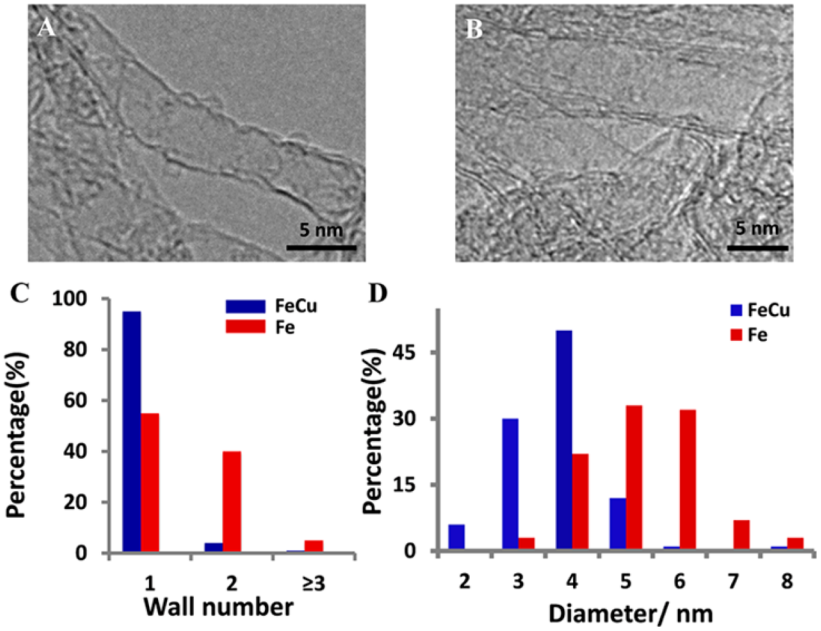

Figure 2. TEM characterization of V-CNTs grown by Fe and Fe−Cu catalyst. TEM images of CNTs grown on (A) Fe/Al_2O_3 catalyst and (B) Fe/0.1 mM $CuCl_2/Al_2O_3$ catalyst. (C) The histograms of wall-number distribution of the V-CNTs grown from Fe and Fe−Cu catalysts. (D) Diameter distribution of CNTs grown on Fe and Fe−Cu catalysts. A total 60 CNTs and 65 CNTs were counted for samples grown on Fe and Fe−Cu catalysts, respectively.

into water to dissolve NaCl, and a copper TEM grid was used to fish out the Fe/Al_2O_3 or $Fe/Cu/Al_2O_3$ film.

Characterization. The CNTs were characterized by scanning electron microscopy (SEM, Hitachi S4800 field emission, Japan) operating at 1.0 kV and by HRTEM using a Tecnai F20 operating at 200 kV. HRTEM samples were prepared by dispersing a section of the CNT forest in ethanol with sonication for 1 h and then placing one drop of the suspension onto a 300 mesh Cu grid with holey carbon coated film. Raman spectroscopy was done with a Horiba HR800 Raman system excited by a 633 nm He−Ne laser with a laser spot size of ~1 μm^2. The catalyst NPs were characterized by atomic force microscopy (AFM, Veeco NanoScope IIIA, Veeco Co.) operated in the tapping mode and HRTEM operating at 200 kV.

RESULTS AND DISCUSSION

Differences in both the morphology of the CNT forest and properties of the CNTs were brought by introducing Cu into the Fe/Al_2O_3 catalyst system. Vertically aligned, densely packed arrays of CNTs could be obtained by using both Fe and Fe−Cu catalysts, as shown in Figure 1, except that the Fe−Cu catalyst grew slightly shorter arrays. The qualities of the V-CNTs were primarily examined by resonant Raman spectroscopy. The ratio between the defect induced D-band and the tangential G-band Raman modes has been well-accepted as an indicator of the quality of the CNTs, as well as a reflection for the content of the SWNTs.[32] The D/G ratio decreased as the amount of Cu introduced increased, which indicates the better quality of CNTs grown by Fe−Cu catalysts. Nonetheless, even with a high concentration of $CuCl_2$ solution introduced, the D/G ratio was still relatively high, which is commonly observed for large-diameter V-SWNT arrays synthesized by water-assisted CVD.[17] The abundance of radial breathing mode (RBM) peaks is an important indicator of the presence of SWNTs. As seen from Figure 1C, weak RBM peaks around 200 cm^{-1} were obtained from Fe grown sample, while more RBM peaks were detected when a small amount of Cu was introduced. As the concentration of $CuCl_2$ solution became higher, more RBM peaks with stronger intensities appeared. Although this observation means that high percentage of SWNTs exists in the Fe/10 mM $CuCl_2$ grown samples, the height of the forest was too short to make a fair comparison with the Fe grown V-CNTs.

It is worth mentioning that the RBM peaks of SWNTs with diameter larger than 2 nm are too weak to be detected by Raman spectroscopy. However, large-diameter SWNTs could probably exist in our samples, which is easy to determine by HRTEM. TEM images in Figure 2A,B revealed that V-CNTs grown on Fe and Fe−Cu catalysts contain a high portion of SWNTs and the Fe−Cu catalyst had a better wall-number selectivity. As exemplified by corresponding histograms (Figure 2C), a SWNT content of 93% was obtained for V-CNTs grown from Fe−Cu catalyst, and a SWNT content of 50% and a DWNT content of 40% were obtained for V-CNTs grown by Fe catalyst. Statistics on the diameter (Figure 2D) showed that most of the tube diameters for both systems are larger than 3 nm, and the mean diameter was 4 and 5 nm for Fe−Cu and Fe catalysts, respectively. The slightly twisted tube shape of the SWNTs was believed to be caused by the sonication during the TEM sample preparation. In addition, the single graphitic layer and the large tube diameter together made the rigidity of these SWNTs lower than that of small-diameter SWNTs, which could even cause collapse of the tubular structure.[33]

Thus, two differences have been made by introducing Cu into the Fe/Al_2O_3 system, which are (i) lowering the height of the V-CNTs but improving their quality; and (ii) increasing the portion of SWNTs significantly but inducing little impact on the diameter distribution. It is reasonable to attribute both results to the change of catalyst properties by the addition of Cu. Our first concern is the effect on the catalyst particle size and its areal density. A research reported by Hata et al. showed

DOI: 10.1021/acs.jpcc.5b12602
J. Phys. Chem. C 2016, 120, 11163−11169

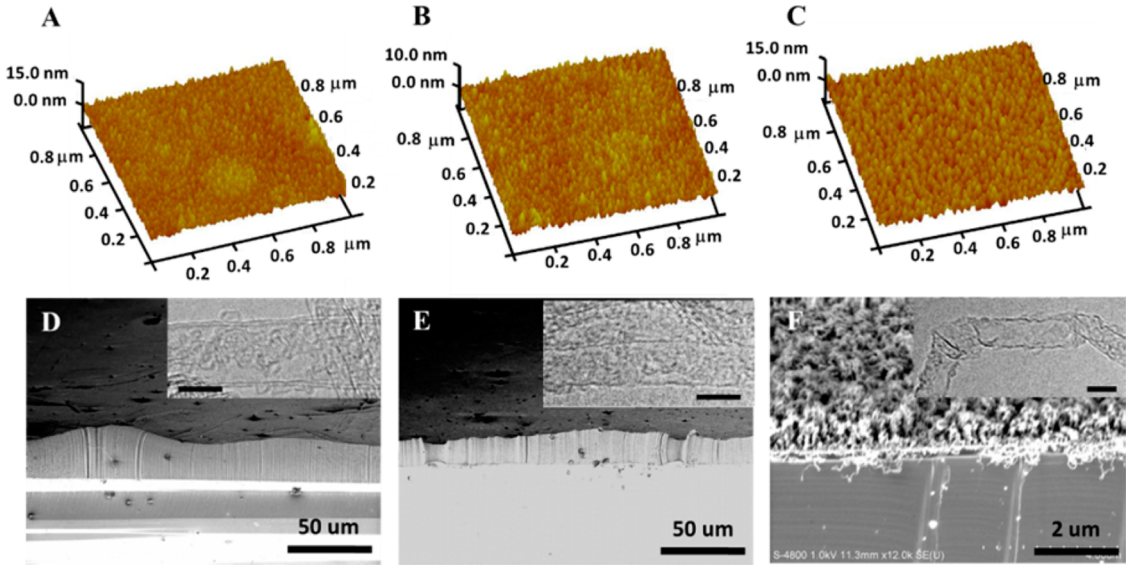

Figure 3. Effect of introduction of Cu on the surface morphology of annealed metal catalyst films and the growth of V-CNTs. AFM 3D images of Fe/Al_2O_3 (A), Fe/0.1 mM $CuCl_2/Al_2O_3$ (B), and Fe/3 mM $CuCl_2/Al_2O_3$ (C) catalysts undergoing the annealing but not the growth stage. SEM images of V-CNTs grown on Fe/Al_2O_3 (D), Fe/0.1 mM $CuCl_2/Al_2O_3$ (E), and Fe/3 mM $CuCl_2/Al_2O_3$ catalyst (F), respectively. Insets in parts D–F are the corresponding TEM images for the CNTs.

that the mean diameter of the V-CNTs is closely related to the thickness of the Fe catalyst film.[13] The reason is that thin metal films fragmented into smaller catalytic particles, which grow CNTs with smaller diameter, whereas thick metal films produce large-diameter CNTs for the same reason. We checked the size and areal density of the catalyst NPs undergoing only the annealing process but not the growth section by AFM. These samples were fast cooled to preserve the size, shape, and crystalline structure of the catalyst NPs to the utmost.

Three-dimensional plots of the surface morphology of Fe and Fe–Cu catalysts with different amounts of Cu introduced are shown in Figure 3A–C. Addition of 0.1 mM $CuCl_2$ solution increased the density of the catalyst without forming larger particles. As the concentration of the $CuCl_2$ solution increased to 3 mM, the density of the NPs became lower, and the size of the NPs became obviously bigger than that of pure Fe catalyst NPs. Surface roughness analysis was performed to give a quantitative evaluation of the particle size distribution. The value of the root-mean-square (Rms) roughness Rq for these three catalysts was 1.17 nm for Rq (Fe), 0.982 nm for Rq (Fe/0.1 mM Cu), and 1.56 nm for Rq (Fe/3 mM Cu), respectively. From the definition of Rq, the Rms average of height deviations taken from the mean data plane, expressed as $Rq = [(1/N)\sum Z_i^2]^{1/2}$, one can tell that Rq actually reflects the size difference as well as the average size of the NPs in this system. This observation indicates that small amount of Cu could restrain the diffusion of Fe NPs and facilitate the formation of small catalytic NPs. By contrast, when more Cu was introduced, the average particle size increased. Meanwhile, smaller sizes of the NPs means tightly packed layers of catalyst nanoparticles, which are essential for the V-CNT growth, especially for SWNTs whose stiffness is generally lower than that of DWCNTs or FWCNTs.[34,35] Apparently the high-density small-size NPs were more favorable for catalyzing growth of V-SWNTs. Small Cu NPs prepared from precursor solution have been proven to be a good catalyst for growing horizontally aligned SWNTs.[36] However, it is speculated that the Cu NPs formed by this way were not large enough to serve as an effective catalyst for the growth of V-SWNTs. Instead, the Cu species nucleated themselves and occupied certain surface area, making the density of the active catalyst NPs become lower. With the "crowding effect" not statistically realized, the direct interactions between the tubes and the substrate that would alter or hinder the growth of the nanotubes leading to the low-efficiency growth of SWNTs in a vertical arrangement by corresponding $Cu/Fe/Al_2O_3$ catalysts (Figure 3F).[35]

TEM characterization on the annealed Al_2O_3 supported catalyst was done to get further information about the detailed structure of the NPs and influence of Cu on the formation of the structures. As shown in Figure 4, Fe–Cu catalyst formed evidently higher density of NPs than Fe catalyst, which confirms the results obtained by AFM. By looking into the shape of the NPs, it is found that pure Fe film fragmented into separate NPs with a round shape, while Fe–Cu catalyst usually formed small clusters composed of several ultrafine irregular-shaped NPs. Previous work showed that high areal density of small-size NPs is essential for preferential growth of SWNTs.[11,37,38] However, at high temperature, NPs are prohibited from maintaining such a state by two processes. Small NPs tend to aggregate to form larger ones, and the metal atoms could diffuse into the underlying support layer.[39] These two processes lead to only low density of large NPs being left in a situation similar to that of Figure 4A, which is not beneficial to the growth of small-diameter CNTs; during the growth, these processes are believed to be the main reasons for the termination of the growth.[20] This fact indicates that the introduction of Cu helps to stabilize the ultrasmall NPs, which is the active catalyst for the SWNT growth. It is worth noticing that when Cu was introduced, although the NPs had different sizes and shapes, they can still catalyze the growth of uniform SWNTs. This result suggests that there must be factors other than the size and shape of the NPs that determines the special catalyzing behavior.

The growth efficiency, as well as the composition of CNT type, has been proven to be related to the redox state of the catalyst. It has been reported that the most reduced Fe catalyst

DOI: 10.1021/acs.jpcc.5b12602
J. Phys. Chem. C 2016, 120, 11163–11169

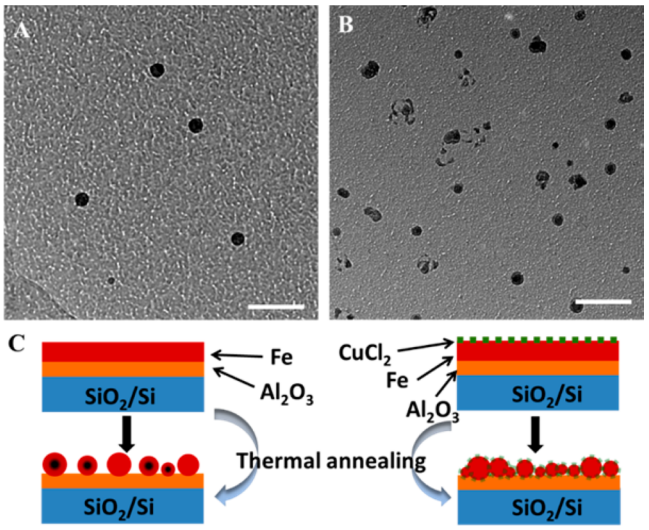

Figure 4. (A, B) TEM characterization results of the Fe and Fe−Cu catalyst NPs derived from Fe (A) and Fe/0.1 mM $CuCl_2$ (B) catalyst films after annealing under Ar−H_2 atmosphere at 750 °C for 40 min. Both catalysts were supported on 50 nm thick Al_2O_3 film. Both scale bars correspond to 200 nm. (C) Schematics showing how the addition of Cu affected the size and density and oxidation state of Fe catalyst NPs. Little black parts within some of the NPs in Fe/Al_2O_3 system represent the incompletely reduced Fe phase. Schematics are not to scale.

produced small-diameter CNTs with highest efficiency, while the least reduced FeO_x yielded larger diameter nanotubes with low yield.[40] To examine the effect of redox state on the growth in our system, we managed to examine the fine structures of the NPs under HRTEM by reducing the thickness of the Al_2O_3 layer down to 10 nm. Typical structures of NPs formed by annealing Fe and Fe−Cu catalyst film were shown in Figure S1A,B. In the Fe−Cu system, NPs composed of only single-phase Fe_2O_3 (hematite, α-Fe_2O_3) were often observed, while the Fe catalyst system contained more NPs composed of a mixture of Fe_2O_3 and Fe_3O_4.[41] It has been found that, under the annealing condition, the reduction of Fe_2O_3 to metallic Fe^0 should follow a two-step reaction sequence, which evolves through Fe_3O_4.[40,42] Since Fe_2O_3 is the thermodynamically stable form of Fe under ambient conditions,[43] it is possible that the single-phase Fe_2O_3 in the Fe/Cu system was converted from completely reduced metallic Fe after the exposure to air. On the contrary, the observation of the kinetically stable Fe_3O_4 phase in the Fe system indicates an incomplete reduction where Fe_3O_4 is still present after the annealing process. A related study on the supported Fe−Cu catalyst in Fischer−Tropsch synthesis (FTS) system revealed that the reduction from Fe_2O_3 to Fe^0 was made fast and complete with Cu addition, whereas the Fe_3O_4 phase existed even after being treated in reductive atmosphere without Cu addition.[42] These facts suggested that by facilitating the formation of catalytically active Fe^0 state, addition of Cu promotes the growth of SWNTs.

On the basis of the observation and analysis above, a model describing how Cu addition affects the size, density, and the oxidation state is proposed. In this model, the thin metal film breaks up into catalytic NPs, and then experienced diffusion both on the surface and into the supporting layer before forming a state suitable for catalyzing CNT nucleation and growth. Without the presence of Cu, Fe film formed low-density and incomplete reduced NPs. However, the introduction of a small amount of Cu not only restricts the diffusion of Fe, but also facilitates the reduction of Fe_2O_3 to Fe^0, which is the most desirable catalyst state for efficient SWNT growth.

To help elucidate the role of Cu, Al_2O_3 and Ni were chosen as representative metal oxide and metal, and deposited onto the surface of Fe/Al_2O_3 respectively. As oxide, Al_2O_3 is supposed to have a size confinement effect but not promote the reduction for Fe nanoparticles. Ni is known as another catalytic metal for CNT growth and is supposed to increase the growth efficiency of the system. It was found that neither of the two catalysts was able to produce the SWNT dominant V-CNT array (Figure S2). This observation confirmed that both the physical confinement and reduction promotion are essential for the selective growth, and were provided by Cu simultaneously.

Following the concept of this model, we designed a new catalyzing system to selectively grow V-DWNTs. It has been revealed by Chen et al. that the "sweet spot" for V-DWNT growth is different from that of the V-SWNTs, with the "sweet spot" for V-DWNT corresponding to large catalyst size.[35] The NPs needed for growing the V-DWNT dominant sample is supposed to be larger than the ones needed for the SWNT forest. To obtain larger catalyst particles that are uniformly and fully reduced, we introduced more Cu by thermal evaporation. The catalyst with Cu layer deposited was found to be unable to produce V-CNT arrays until the Cu layer is thicker than 0.8 nm. Using the (0.8 nm Cu)/Fe/Al_2O_3 catalyst, we synthesized V-CNTs with height of ~30 μm, and a DWNT content of ~85% (Figure 5). It can be easily seen from the AFM images

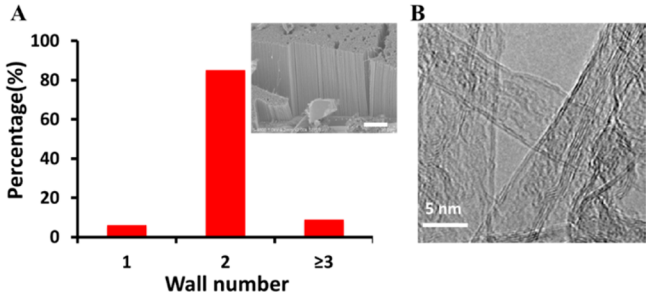

Figure 5. V-CNT growth on the 0.8 nm Cu/Fe/Al_2O_3 catalyst. (A). Statistics on the wall-number distribution of the V-CNTs. Inset is the SEM image of the V-CNT arrays. Scale bar in insets corresponds to 10 μm. (B) Typical TEM images of V-CNTs. A total of ~70 CNTs were counted for the statistics.

shown in Figure S4A that densely distributed large-size NPs formed after annealing. Intriguingly, when the thickness of Cu layer was increased to 1.0 nm, the forest grown was mainly composed of few-walled CNTs (FWNTs) (Figure S3). These results indicated that Cu nanoparticles formed from the deposited Cu layer actually acted as active catalyst for the CNT growth. However, too much Cu would result in the formation of large Cu nanoparticles, which are shown here to be more suitable for FWNT growth. Therefore, we believe that introduction of Cu indeed helps achieve the most efficient catalyst reduction process. Moreover, the amount of Cu introduced is considered important because catalytic efficiency is related to the size of the NPs.

CONCLUSIONS

We have demonstrated the preferential growth of dense arrays of vertically aligned SWNTs and DWNTs using the CVD

DOI: 10.1021/acs.jpcc.5b12602
J. Phys. Chem. C 2016, 120, 11163−11169

method, respectively. It was found that introduction of Cu into the Fe/Al_2O_3 catalyzing system inhibited diffusion of Fe NPs and facilitated the full reduction of Fe catalyst, with the former determining the high-density and small-size NPs, and the latter one having made the NPs have uniform oxidation state regardless of their sizes. Subsequently, either V-SWNTs or V-DWNTs could be controllably synthesized with high selectivity. A clear relationship between catalyst property and CNT structure is considered to be crucial toward the goal of controlled growth of CNTs via catalyst-engineering strategies. Further optimization on the fabrication technology of the Fe−Cu or other bimetallic catalysts, as well as the CVD growth conditions, is going to promote the growth of V-CNTs with more controlled structure and properties such as diameter, electrical property, and even chirality.

■ ASSOCIATED CONTENT

Supporting Information

The Supporting Information is available free of charge on the ACS Publications website at DOI: 10.1021/acs.jpcc.5b12602.

High-resolution TEM characterization of Fe and Fe−Cu catalyst, growth result by Ni/Fe/Al_2O_3 and Al_2O_3/Fe/Al_2O_3 catalysts, and influence of the thickness and sequence of Cu deposition on V-CNT growth (PDF)

■ AUTHOR INFORMATION

Corresponding Author

*E-mail: jinzhang@pku.edu.cn.

Notes

The authors declare no competing financial interest.

■ ACKNOWLEDGMENTS

This work was supported by NSFC (21233001, 51272006, and 51432002) and MOST (2011CB932601).

■ REFERENCES

(1) Coleman, J. N.; Khan, U.; Blau, W. J.; Gun'ko, Y. K. Small but Strong: A Review of the Mechanical Properties of Carbon Nanotube−Polymer Composites. *Carbon* **2006**, *44*, 1624−1652.

(2) Kim, P.; Shi, L.; Majumdar, A.; McEuen, P. Thermal Transport Measurements of Individual Multiwalled Nanotubes. *Phys. Rev. Lett.* **2001**, *87*, 215502.

(3) Kordas, K.; Tóth, G.; Moilanen, P.; Kumpumäki, M.; Vähäkangas, J.; Uusimäki, A.; Vajtai, R.; Ajayan, P. Chip Cooling with Integrated Carbon Nanotube Microfin Architectures. *Appl. Phys. Lett.* **2007**, *90*, 123105.

(4) Wu, Z.; Chen, Z.; Du, X.; Logan, J. M.; Sippel, J.; Nikolou, M.; Kamaras, K.; Reynolds, J. R.; Tanner, D. B.; Hebard, A. F. Transparent, Conductive Carbon Nanotube Films. *Science* **2004**, *305*, 1273−1276.

(5) Green, A. A.; Hersam, M. C. Processing and Properties of Highly Enriched Double-Wall Carbon Nanotubes. *Nat. Nanotechnol.* **2009**, *4*, 64−70.

(6) Dresselhaus, M. S.; Dresselhaus, G.; Eklund, P.; Rao, A. *Carbon Nanotubes*; Springer, 2000.

(7) Dalton, A. B.; Collins, S.; Munoz, E.; Razal, J. M.; Ebron, V. H.; Ferraris, J. P.; Coleman, J. N.; Kim, B. G.; Baughman, R. H. Super-Tough Carbon-Nanotube Fibres. *Nature* **2003**, *423*, 703−703.

(8) Ericson, L. M.; Fan, H.; Peng, H.; Davis, V. A.; Zhou, W.; Sulpizio, J.; Wang, Y.; Booker, R.; Vavro, J.; Guthy, C. Macroscopic, Neat, Single-Walled Carbon Nanotube Fibers. *Science* **2004**, *305*, 1447−1450.

(9) Baughman, R. H.; Zakhidov, A. A.; de Heer, W. A. Carbon Nanotubes - the Route toward Applications. *Science* **2002**, *297*, 787−792.

(10) Tsai, T.; Lee, C.; Tai, N.; Tuan, W. Transfer of Patterned Vertically Aligned Carbon Nanotubes onto Plastic Substrates for Flexible Electronics and Field Emission Devices. *Appl. Phys. Lett.* **2009**, *95*, 013107.

(11) Mizuno, K.; Ishii, J.; Kishida, H.; Hayamizu, Y.; Yasuda, S.; Futaba, D. N.; Yumura, M.; Hata, K. A Black Body Absorber from Vertically Aligned Single-Walled Carbon Nanotubes. *Proc. Natl. Acad. Sci. U. S. A.* **2009**, *106*, 6044−6047.

(12) Yu, M.; Funke, H. H.; Falconer, J. L.; Noble, R. D. High Density, Vertically-Aligned Carbon Nanotube Membranes. *Nano Lett.* **2009**, *9*, 225−229.

(13) Futaba, D. N.; Hata, K.; Yamada, T.; Hiraoka, T.; Hayamizu, Y.; Kakudate, Y.; Tanaike, O.; Hatori, H.; Yumura, M.; Iijima, S. Shape-Engineerable and Highly Densely Packed Single-Walled Carbon Nanotubes and Their Application as Super-Capacitor Electrodes. *Nat. Mater.* **2006**, *5*, 987−994.

(14) Yamada, T.; Namai, T.; Hata, K.; Futaba, D. N.; Mizuno, K.; Fan, J.; Yudasaka, M.; Yumura, M.; Iijima, S. Size-Selective Growth of Double-Walled Carbon Nanotube Forests from Engineered Iron Catalysts. *Nat. Nanotechnol.* **2006**, *1*, 131−136.

(15) Amama, P. B.; Pint, C. L.; Kim, S. M.; McJilton, L.; Eyink, K. G.; Stach, E. A.; Hauge, R. H.; Maruyama, B. Influence of Alumina Type on the Evolution and Activity of Alumina-Supported Fe Catalysts in Single-Walled Carbon Nanotube Carpet Growth. *ACS Nano* **2010**, *4*, 895−904.

(16) Zhong, G.; Warner, J. H.; Fouquet, M.; Robertson, A. W.; Chen, B.; Robertson, J. Growth of Ultrahigh Density Single-Walled Carbon Nanotube Forests by Improved Catalyst Design. *ACS Nano* **2012**, *6*, 2893−2903.

(17) Han, Z. J.; Ostrikov, K. Uniform, Dense Arrays of Vertically Aligned, Large-Diameter Single-Walled Carbon Nanotubes. *J. Am. Chem. Soc.* **2012**, *134*, 6018−6024.

(18) Hata, K.; Futaba, D. N.; Mizuno, K.; Namai, T.; Yumura, M.; Iijima, S. Water-Assisted Highly Efficient Synthesis of Impurity-Free Single-Walled Carbon Nanotubes. *Science* **2004**, *306*, 1362−1364.

(19) Yamada, T.; Maigne, A.; Yudasaka, M.; Mizuno, K.; Futaba, D. N.; Yumura, M.; Iijima, S.; Hata, K. Revealing the Secret of Water-Assisted Carbon Nanotube Synthesis by Microscopic Observation of the Interaction of Water on the Catalysts. *Nano Lett.* **2008**, *8*, 4288−4292.

(20) Amama, P. B.; Pint, C. L.; McJilton, L.; Kim, S. M.; Stach, E. A.; Murray, P. T.; Hauge, R. H.; Maruyama, B. Role of Water in Super Growth of Single-Walled Carbon Nanotube Carpets. *Nano Lett.* **2009**, *9*, 44−49.

(21) Li, S.; Hou, P.; Liu, C.; Gao, L.; Liu, B.; Zhang, L.; Song, M.; Cheng, H.-M. Wall-Number Selective Growth of Vertically Aligned Carbon Nanotubes from Fept Catalysts: A Comparative Study with Fe Catalysts. *J. Mater. Chem.* **2012**, *22*, 14149−14154.

(22) Nishino, H.; Yasuda, S.; Namai, T.; Futaba, D. N.; Yamada, T.; Yumura, M.; Iijima, S.; Hata, K. Water-Assisted Highly Efficient Synthesis of Single-Walled Carbon Nanotubes Forests from Colloidal Nanoparticle Catalysts. *J. Phys. Chem. C* **2007**, *111*, 17961−17965.

(23) Murakami, Y.; Chiashi, S.; Miyauchi, Y.; Hu, M.; Ogura, M.; Okubo, T.; Maruyama, S. Growth of Vertically Aligned Single-Walled Carbon Nanotube Films on Quartz Substrates and Their Optical Anisotropy. *Chem. Phys. Lett.* **2004**, *385*, 298−303.

(24) Hiraoka, T.; Yamada, T.; Hata, K.; Futaba, D. N.; Kurachi, H.; Uemura, S.; Yumura, M.; Iijima, S. Synthesis of Single-and Double-Walled Carbon Nanotube Forests on Conducting Metal Foils. *J. Am. Chem. Soc.* **2006**, *128*, 13338−13339.

(25) Orbaek, A. W.; Owens, A. C.; Crouse, C. C.; Pint, C. L.; Hauge, R. H.; Barron, A. R. Single Walled Carbon Nanotube Growth and Chirality Dependence on Catalyst Composition. *Nanoscale* **2013**, *5*, 9848−9859.

(26) Hong, G.; Chen, Y.; Li, P.; Zhang, J. Controlling the Growth of Single-Walled Carbon Nanotubes on Surfaces Using Metal and Non-Metal Catalysts. *Carbon* **2012**, *50*, 2067−2082.

(27) Yang, F.; Wang, X.; Zhang, D.; Yang, J.; Luo, D.; Xu, Z.; Wei, J.; Wang, J.-Q.; Xu, Z.; Peng, F.; et al. Chirality-Specific Growth of Single-

DOI: 10.1021/acs.jpcc.5b12602
J. Phys. Chem. C 2016, 120, 11163−11169

Walled Carbon Nanotubes on Solid Alloy Catalysts. *Nature* **2014**, *510*, 522−524.
(28) Bachilo, S. M.; Balzano, L.; Herrera, J. E.; Pompeo, F.; Resasco, D. E.; Weisman, R. B. Narrow (N, M)-Distribution of Single-Walled Carbon Nanotubes Grown Using a Solid Supported Catalyst. *J. Am. Chem. Soc.* **2003**, *125*, 11186−11187.
(29) He, M.; Chernov, A. I.; Fedotov, P. V.; Obraztsova, E. D.; Sainio, J.; Rikkinen, E.; Jiang, H.; Zhu, Z.; Tian, Y.; Kauppinen, E. I.; et al. Predominant (6,5) Single-Walled Carbon Nanotube Growth on a Copper-Promoted Iron Catalyst. *J. Am. Chem. Soc.* **2010**, *132*, 13994−13996.
(30) He, M.; Liu, B.; Chernov, A. I.; Obraztsova, E. D.; Kauppi, I.; Jiang, H.; Anoshkin, I.; Cavalca, F.; Hansen, T. W.; Wagner, J. B.; et al. Growth Mechanism of Single-Walled Carbon Nanotubes on Iron−Copper Catalyst and Chirality Studies by Electron Diffraction. *Chem. Mater.* **2012**, *24*, 1796−1801.
(31) Chiang, W.-H.; Sankaran, R. M. Linking Catalyst Composition to Chirality Distributions of as-Grown Single-Walled Carbon Nanotubes by Tuning Ni_x Fe_{1-X} Nanoparticles. *Nat. Mater.* **2009**, *8*, 882−886.
(32) Costa, S.; Borowiak-Palen, E.; Kruszynska, M.; Bachmatiuk, A.; Kalenczuk, R. Characterization of Carbon Nanotubes by Raman Spectroscopy. *Mater. Sci-Poland* **2008**, *26*, 433−441.
(33) Zhang, C.; Bets, K.; Lee, S. S.; Sun, Z.; Mirri, F.; Colvin, V. L.; Yakobson, B. I.; Tour, J. M.; Hauge, R. H. Closed-Edged Graphene Nanoribbons from Large-Diameter Collapsed Nanotubes. *ACS Nano* **2012**, *6*, 6023−6032.
(34) Orbaek, A. W.; Owens, A. C.; Barron, A. R. Increasing the Efficiency of Single Walled Carbon Nanotube Amplification by Fe−Co Catalysts through the Optimization of Ch_4/H_2 Partial Pressures. *Nano Lett.* **2011**, *11*, 2871−2874.
(35) Chen, G.; Davis, R. C.; Futaba, D. N.; Sakurai, S.; Kobashi, K.; Yumura, M.; Hata, K. A Sweet Spot for Highly Efficient Growth of Vertically Aligned Single-Walled Carbon Nanotube Forests Enabling Their Unique Structures and Properties. *Nanoscale* **2016**, *8*, 162−171.
(36) Ding, L.; Yuan, D.; Liu, J. Growth of High-Density Parallel Arrays of Long Single-Walled Carbon Nanotubes on Quartz Substrates. *J. Am. Chem. Soc.* **2008**, *130*, 5428−5429.
(37) Cheung, C. L.; Kurtz, A.; Park, H.; Lieber, C. M. Diameter-Controlled Synthesis of Carbon Nanotubes. *J. Phys. Chem. B* **2002**, *106*, 2429−2433.
(38) Chen, R. J.; Zhang, Y.; Wang, D.; Dai, H. Noncovalent Sidewall Functionalization of Single-Walled Carbon Nanotubes for Protein Immobilization. *J. Am. Chem. Soc.* **2001**, *123*, 3838−3839.
(39) Sakurai, S.; Nishino, H.; Futaba, D. N.; Yasuda, S.; Yamada, T.; Maigne, A.; Matsuo, Y.; Nakamura, E.; Yumura, M.; Hata, K. Role of Subsurface Diffusion and Ostwald Ripening in Catalyst Formation for Single-Walled Carbon Nanotube Forest Growth. *J. Am. Chem. Soc.* **2012**, *134*, 2148−2153.
(40) Teblum, E.; Gofer, Y.; Pint, C. L.; Nessim, G. D. Role of Catalyst Oxidation State in the Growth of Vertically Aligned Carbon Nanotubes. *J. Phys. Chem. C* **2012**, *116*, 24522−24528.
(41) Peng, Y.; Park, C.; Laughlin, D. E. Fe_3 O_4 Thin Films Sputter Deposited from Iron Oxide Targets. *J. Appl. Phys.* **2003**, *93*, 7957−7959.
(42) de Smit, E.; de Groot, F. M.; Blume, R.; Hävecker, M.; Knop-Gericke, A.; Weckhuysen, B. M. The Role of Cu on the Reduction Behavior and Surface Properties of Fe-Based Fischer−Tropsch Catalysts. *Phys. Chem. Chem. Phys.* **2010**, *12*, 667−680.
(43) Lombardo, J. J.; Lysaght, A. C.; Goberman, D. G.; Chiu, W. K. Effect of Particle Size on Iron Nanoparticle Oxidation State. *Thin Solid Films* **2012**, *520*, 2036−2040.

DOI: 10.1021/acs.jpcc.5b12602
J. Phys. Chem. C 2016, 120, 11163−11169